Electronic Supplementary Material (ESI) for Metallomics.

SUPPORTING INFORMATION

Copper(I) targeting in the Alzheimer's disease context: a first example using the biocompatible PTA ligand

E. Atrian-Blasco, E. Cerrada, A. Conte-Daban, D. Testemale, P. Faller, M. Laguna, and C. Hureau

Ma**terials and methods.**

Aβ16 peptide (sequence DAEFRHDSGYEVHHQK) was bought from GeneCust (Dudelange, Luxembourg) with a 95% purity grade.

Approx. 10 mM stock solution of peptide was prepared by dissolving the powder in milliQ water (resulting pH ~ 2). Peptide concentration was then determined by UV-visible absorption of Tyr10 considered as free tyrosine ($(\varepsilon_{276}-\varepsilon_{296})$ = 1410 $M^{-1}cm^{-1}$).

Human Aβ40 peptide (DAEFRHDSGYEVHHQKLVFFAEDVGSNK-GAIIGLMVGGVV) was bought from GeneCust (Dudelange, Luxembourg) with a 95% purity grade. It was prepared by dissolving the powder in milliQ water and peptide concentration was then determined by UV-visible absorption of Tyr10 considered as free tyrosine ($(\varepsilon_{293}-\varepsilon_{360})$ = 2400 $M^{-1}cm^{-1}$) in NaOH 0.1 M.[1]

Copper solutions: Cu(II) used was from $CuSO_4.5(H_2O)$ and purchased from Sigma. Stock solution of Cu(II) (~1M) was prepared in D_2O.

Hepes buffer (sodium salt of 2-[4-(2-hydroxyethyl)piperazin-1-yl]ethanesulfonic acid) was bought from Fluka (bioluminescence grade).

Phosphate buffer was prepared from K_2HPO_4 and KH_2PO_4 bought from Sigma-Aldrich.

Ascorbate: A stock solution (20 mM) of ascorbate was prepared in milli-Q water at room temperature just before beginning the experiment and was used immediately. Because ascorbate degrades very quickly, a new solution was prepared for each experiment.

CCA: A stock solution of coumarin-3-carboxylic acid (5 mM) was prepared in phosphate (20 mM), NaCl (100 mM) buffer at pH 9 at room temperature. The stock solution was stored at -20°C.

PTA was prepared according to procedures described in ref. [2].

UV-Vis spectroscopy: UV-Vis spectra were recorded on Agilent 8453 UV-Visible.

Fluorescence spectroscopy: Fluorescence spectra were measured by using a Fluostar Optima (BMG Labtech) connected to a personal computer. Thioflavin T, Aβ40, Cu(II) and PTA ligand were mixed in XXX buffer 100 mM pH 7.4 and placed in 96-well microplate. The time course of thioflavin T fluorescence was then measured (Excitation 440 nm ; Emission 490 nm, bandwidth for emission and excitation 10 nm).

NMR: 1D ^1H experiments were recorded on a Bruker Avance 500 spectrometer equipped with a 5 mm triple resonance inverse Z-gradient probe (TBI ^1H, ^{31}P, BB). All chemical shifts are relative to tetramethylsilane. Spectra were collected at 298 K in D_2O. NMR tubes were

prepared under Argon. The $Cu^{I}(A\beta)$ complex state was obtained from the Cu(II) counterpart by reduction with 1.5 equiv. of dithionite according to ref. [3]. Briefly, samples were prepared as follow: the Cu(I) was produced in situ, by direct addition (1.5 equiv.) of fresh made $Na_2S_2O_3$ stock solution (0.1M) into a NMR tube previously degassed with water-saturated Ar containing the peptide and Cu(II) at 1 mM concentration. NMR tube was sealed under Ar, measured as soon as possible to prevent possible oxidation. In such conditions, no broadening due to Cu(II) traces was observed and no significant pH drift due to the addition of $Na_2S_2O_3$ was measured.

EPR: Electron Paramagnetic Resonance (EPR) data were recorded using an Elexsys E 500 Bruker spectrometer, operating at a microwave frequency of approximately 9.5 GHz. All spectra were recorded using a microwave power of 20 mW across a sweep width of 150 mT (centred at 310 mT) with modulation amplitude of 0.5 mT. Experiments were carried out at 110 K using a liquid nitrogen cryostat.

EPR samples were prepared from stock solution of peptide diluted down to 0.2 mM in H_2O. 0.9 equiv. of Cu(II) was added from 0.1 M $Cu(NO_3)_2$ stock solution. Samples were frozen in quartz tube after addition of 10% glycerol as a cryoprotectant and stored in liquid nitrogen until used.

XANES: Cu K-edge XANES (X-ray absorption near edge structure) spectra were recorded at the BM30B (FAME) beamline at the European Synchrotron Radiation Facility (ESRF, Grenoble, France).[4] The storage ring was operated in 7/8+1 mode at 6GeV with a 200mA current. The beam energy was selected using an Si(220) N_2 cryo-cooled double-crystal monochromator with an experimental resolution close to that theoretically predicted (namely ~ 0.5 eV FWHM at the Cu energy).[5] The beam spot on the sample was approximately 300 x 200 μm^2 (H x V, FWHM). Because of the low Cu concentrations, spectra were recorded in fluorescence mode with a 30-element solid state Ge detector (Canberra) in frozen liquid cells in a He cryostat. The temperature was kept at 10 K during data collection to prevent sample damage and slow down possible beam-induced Cu photo-reduction. In addition, to limit this Cu photo-reduction even further, samples are moved at each scan in order for the radiation not to hit the same portion of the sample. The energy was calibrated with Cu metallic foils, such that the maximum of the first derivative was set at 8979. Cu data were collected from 8830 to 8960 eV using 3 eV step of 2 s, from 8960 to 9030 eV using 0.5 eV step of 3 s, and from 9030 to 9300 eV with a k-step of 0.05 $Å^{-1}$ and an increasing time of 2-10 s per step. For each sample three scans were averaged and spectra were background-corrected by a linear

regression through the pre-edge region and a polynomial through the post-edge region and normalized to the edge jump.

Samples for XANES measurements were prepared in presence of 10% of glycerol as cryoprotectant.

Coumarin-3-carboxylic acid assay. 3-CCA was used to detect $HO^{\bullet}$. $HO^{\bullet}$ reacts with 3-CCA to form 7-hydroxy-coumarin-3-carboxylic acid (7-OH-CCA), which is fluorescent at 452 nm upon excitation at 395 nm. The intensity of the fluorescence signal is proportional to the number of 7-OH-CCA molecules formed.

Ascorbate consumption was monitored by UV-Vis. Intensity of the Asc absorption band at λ = 265 nm (ε = 14 500 M-1.cm-1) was monitored as a function of time, in 100 mM phosphate buffer, pH 7.4 containing 100 µM of Asc.

Atomic Force Microscopy (AFM)

Taping-mode AFM imaging was performed in air on a Smart SPM-1000 microscope (AIST-NT, Novato, USA) equipped with a 100µm scanner. Sample solutions (20µM) were deposited on freshly cleaved mica and left for adsorption on the substrate for 10 min. They were then rinsed three times with deionized water to remove salts and loosely bound peptide and dried with compressed N_2 before imaging. Commercial Si cantilevers (NanoWorld, Swizerland) with an elastic modulus of ~42 N m^{-1} were used. All images were acquired as 512 x 512 pixel images at a typical scan rate of 1.0 kHz with a vertical tip oscillation frequency of 250-350 kHz. Representative images of each chemical system (apo-Aβ, Cu^{II}(Aβ), Cu^{II}(Aβ) + 5PTA and Cu^{II}(Aβ) + 20PTA) were obtained by scanning at least 5 different locations on at least two different samples of the same chemical system.

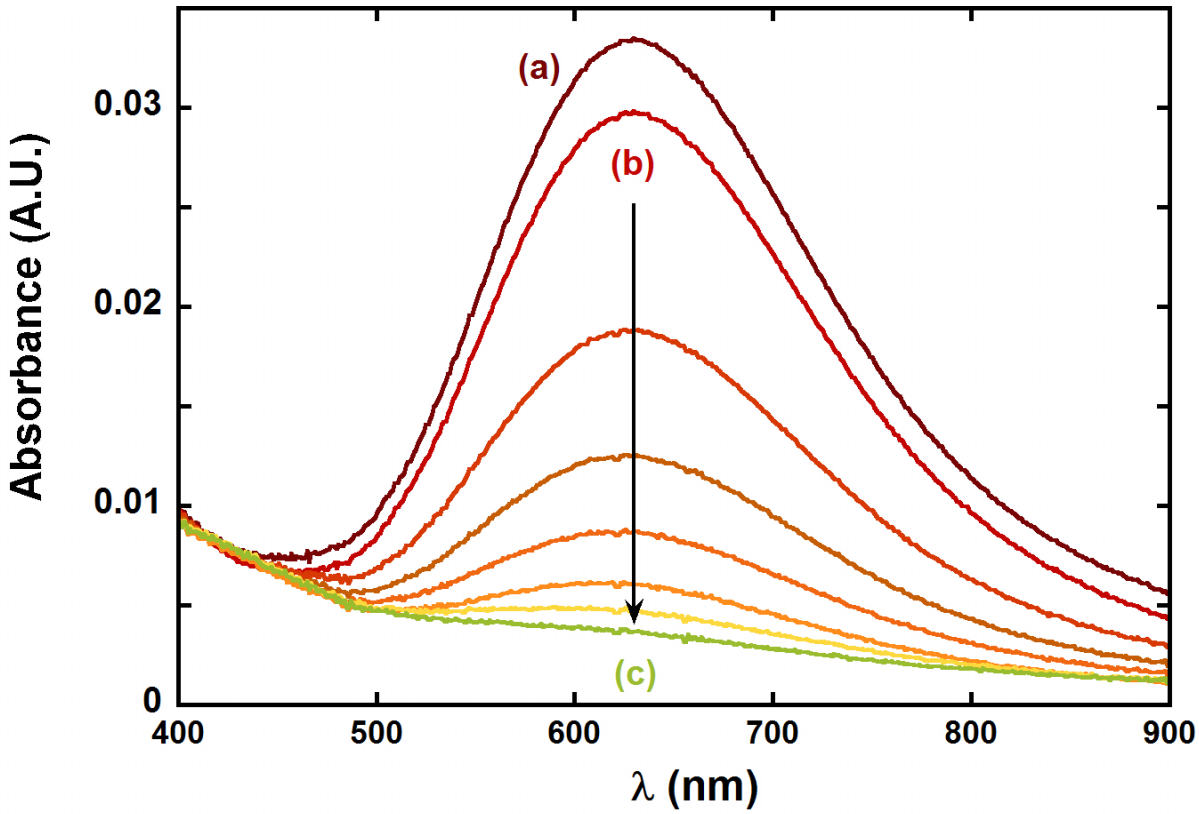

Figure S1. UV-Vis signature of Cu^{II}(Aβ) complex before and after addition of 6 equiv. of PTA as a function of time. (a) before addition of the PTA ligands, and from t = 0 (b) to t = 60 min (c) after addition of the PTA ligands. [Aβ16] = 500 µM, [Cu] = 450 µM, [PTA] = 2.7 mM, Phosphate buffer 50 mM pH 7.4, T = 25°C, ℓ = 1 cm.

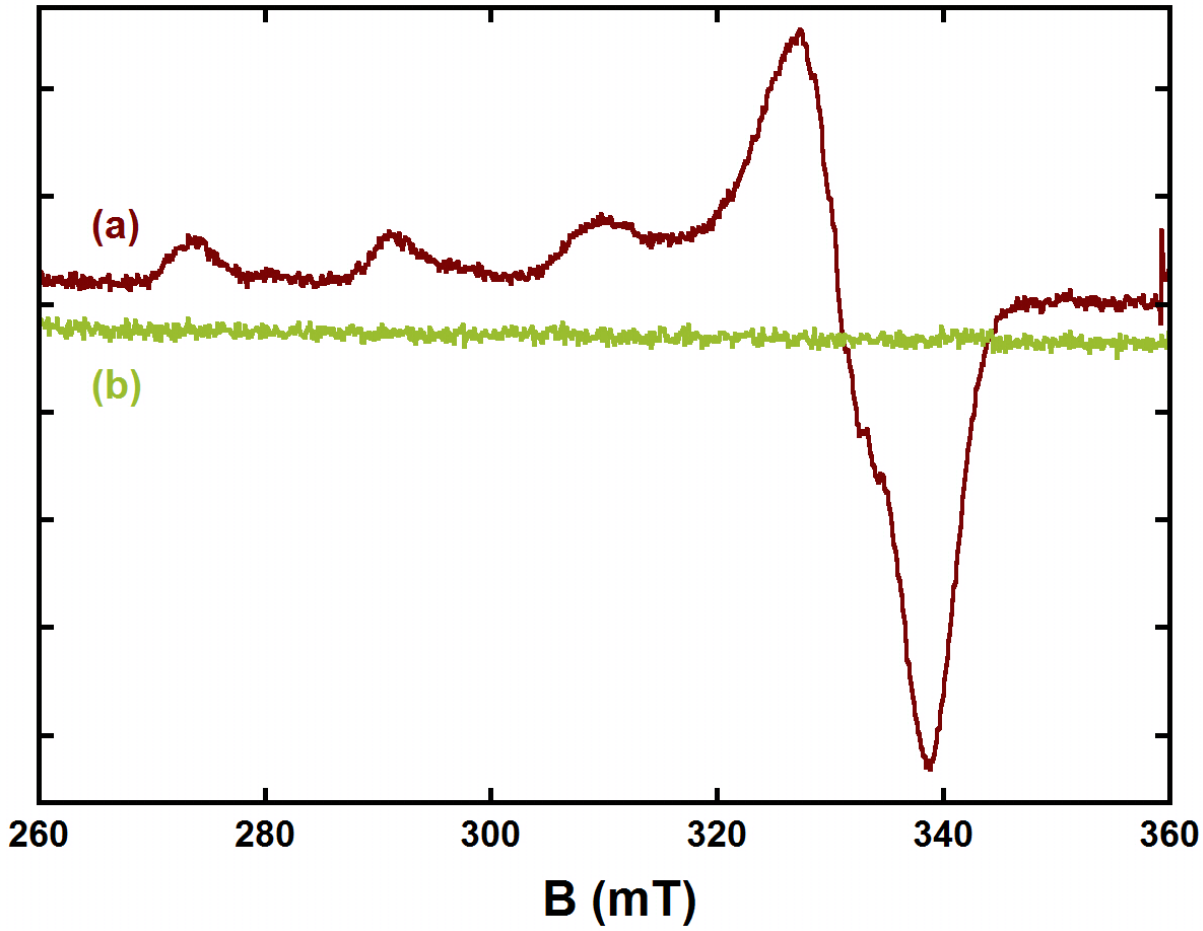

Figure S2. EPR signature of $Cu^{II}(A\beta)$ complex before (a) and after one hour of incubation with 6 PTA equivalents (b). [Aβ16] = 200 μM, [Cu] = 180 μM, [PTA] = 1.4 mM, pH 7.4, *T* = 120 K.

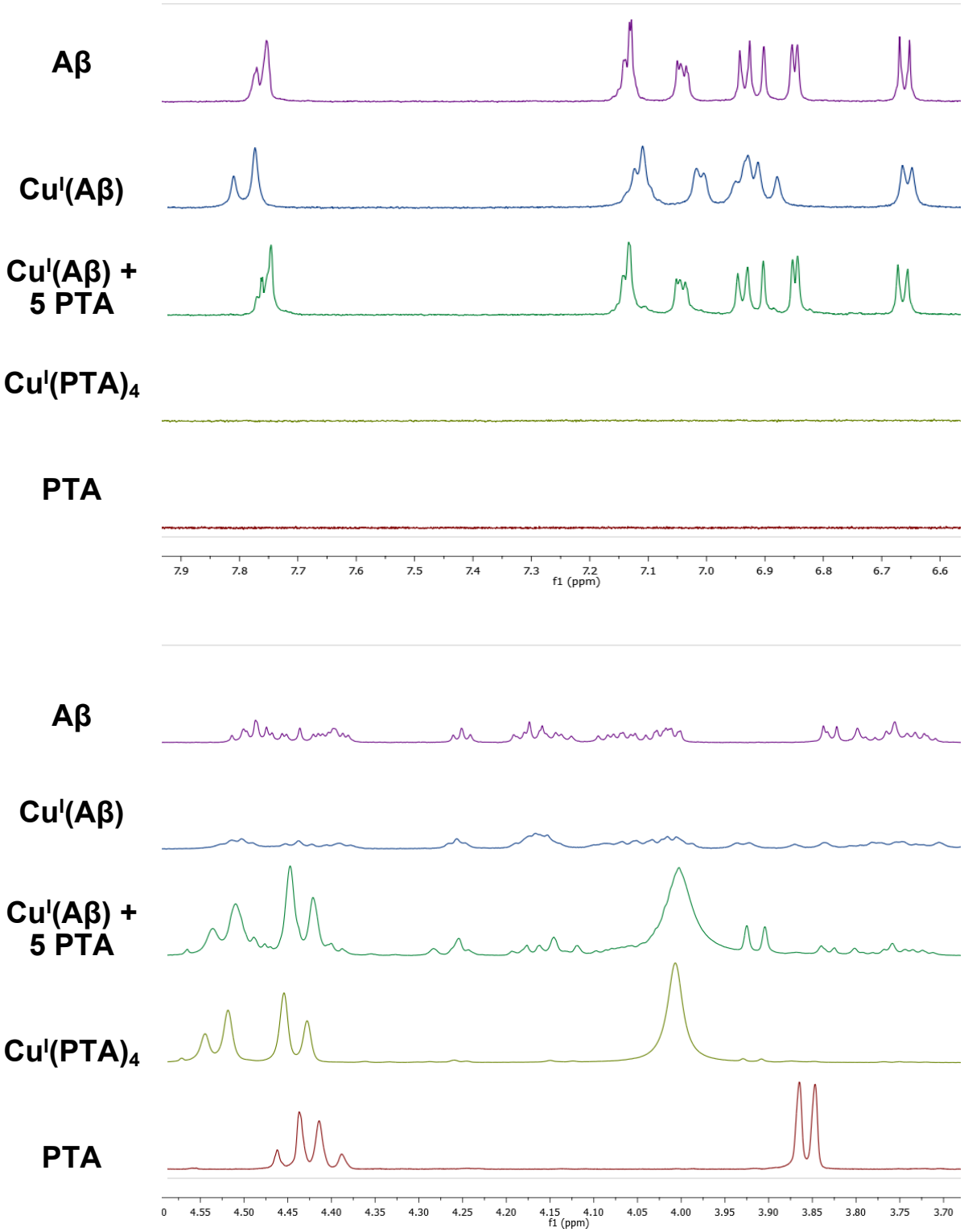

Figure S3. ^{1}H NMR Spectra. From top to bottom: spectra of the Aβ peptide, the Cu^{I}(Aβ) complex prepared as described in ref. [3] and Cu^{I}(Aβ) after addition of 5 equiv. of PTA ligand, of the Cu^{I}(PTA)$_4$ complex and of the PTA ligand. Top: aromatic regions; Bottom: aliphatic regions. [Aβ16] = 1 mM, [Cu^{I}] = 0.9 mM, [PTA] = 5 mM, Phosphate buffer 0.1M. υ = 500 MHz, T = 25°C.

After addition of the PTA ligands to the $Cu^{I}(A\beta)$ species, the NMR signature of both the unbound Aβ and the $Cu^{I}(PTA)_4$ complex are observed.

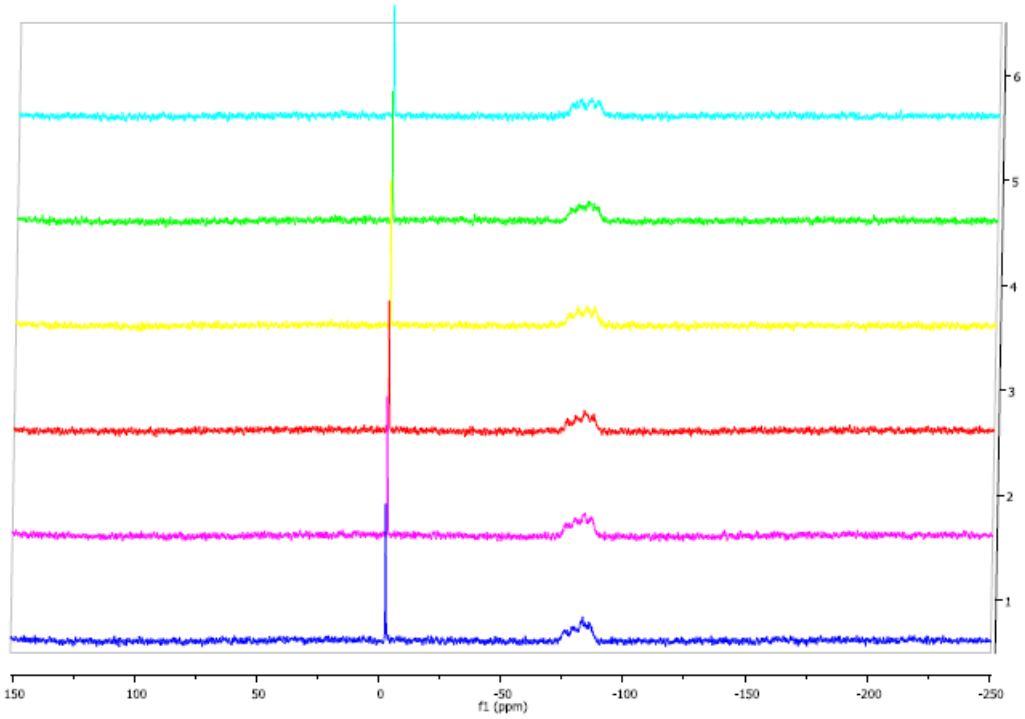

Figure S4. $^{31}P\{^{1}H\}$-NMR spectra of the PTA ligand after addition of Cu(II). [PTA] = 30 mM, [Cu(II)] = 6.7 mM, no buffer, pH = 6.5 (bottom) to 9.5 (top) adjusted by NaOD and D_2SO_4. υ = 500 MHz, T = 25°C.

The PTA oxide signal is at approx. -2 ppm, and the broad signal of $[Cu(PTA)_4]^+$ at -80 ppm. Note that if there is free PTA ligand, we could not see the corresponding singulet, as due to equilibria it would be included in the broad signal at -80 ppm. As it was not possible to buffer the solution using phosphate buffer, experiments were performed on a large pH range and show similar results.

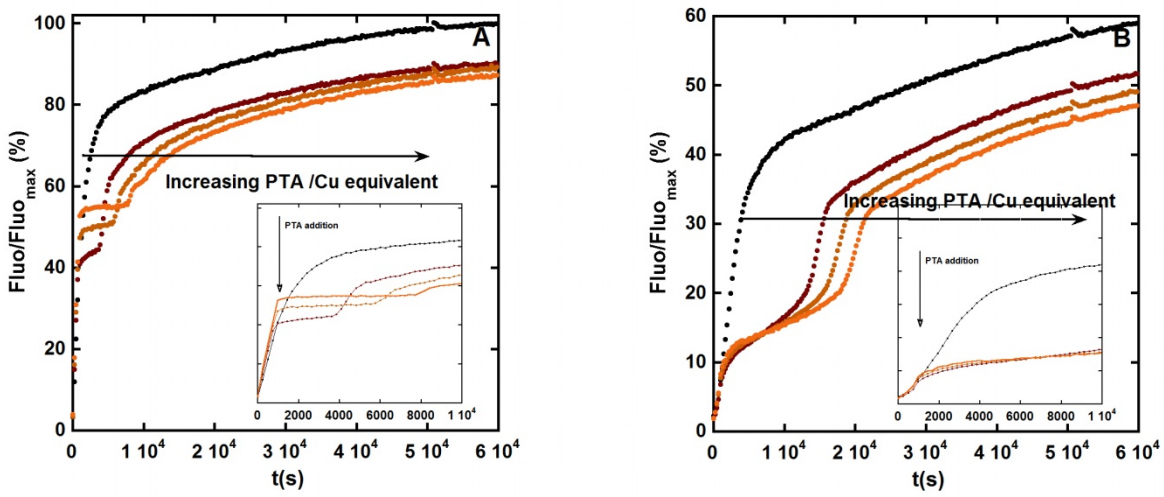

Figure S5. 7-OH-CCA Fluorescence spectra of unbound Cu (panel A) of Cu(Aβ) (panel B) in presence of increasing equivalent of PTA (no PTA added, black dots), 4 equiv. of PTA (brown dots), 5 equiv. of PTA (light brown dots) and 6 equiv. of PTA (orange dots) added at t ~15 min after the start of the ROS production. [Cu^{II}] = 10µM, [Aβ16] = 12 µM, [PTA] = 0, 42, 52, 63 µM, [CCA] = 500 µM, [ascorbate] = 1mM, phosphate buffer, 50mM, pH 7.4, T= 25°C.

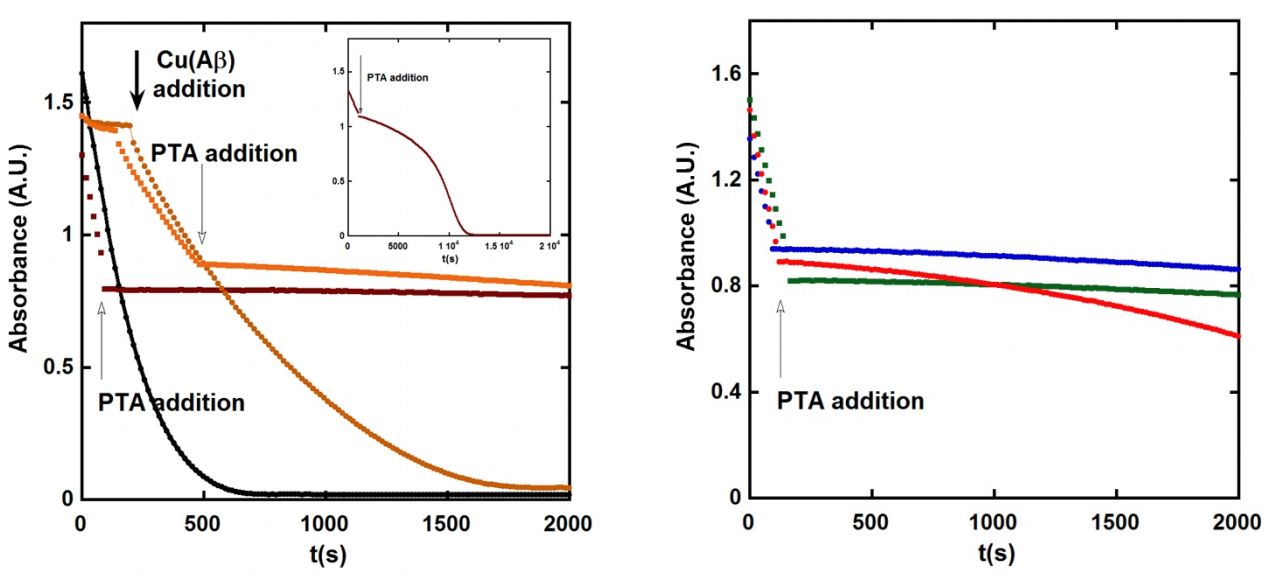

Figure S6. Left: UV-Vis absorption of ascorbate (at 265 nm) as a function of time in presence of unbound Cu before (solid lines, black dots) and after addition of 5 equiv. of PTA (dark brown squares) or of Cu(Aβ) before (solid lines, light brown dots) and after addition of 5 equiv. of PTA (orange squares). Inset: UV-Vis absorption of ascorbate (at 265 nm) as a function of time in presence of Cu(Aβ) after addition of 5 equiv. of PTA. $[Cu^{II}]$ = 10µM, [Aβ16] = 12 µM, [PTA] = 60 µM, [ascorbate] = 100 µM, Hepes 50mM, pH 7.4, T= 25°C. Right: UV-Vis absorption of ascorbate (at 265 nm) as a function of time in presence of unbound Cu before and after addition of 2 (red line), 3 (blue line), and 4 equiv. of PTA (green line). $[Cu^{II}]$ = 10µM, [Aβ16] = 12 µM, [PTA] = 24, 36 and 48 µM, [ascorbate] = 100 µM, Hepes 50mM, pH 7.4

In presence of the PTA ligands, the ascorbate consumption is dramatically slowed down. The same trend as in the HO° experiment is also observed here with a flattening of the slope after the PTA addition that is weaker in presence of Aβ (See full text, Figure 2). In the inset of Figure 5, the sigmoid-like curve observed in the HO° experiment is also present when time necessary to complete the reaction is allowed (Figure S6, left).

In presence of 3 and 4 PTA equivalents, the ascorbate consumption is highly slowed down, which is no more the case with 2 equivalents of PTA. This is in line with a $[Cu(PTA)_3]^+$ air-stable complex (Figure S6, right). Anyway, the $[Cu(PTA)_2]^+$ species remains less efficient in ascorbate consumption than Cu(Aβ).

Note that for experimental reasons (use of a multi-plate fluorimeter but of a single cuvette UV-Vis), it is possible to screen several conditions on long time scale by fluorescence but not by UV-Vis.

Speciation of Cu(I), $[Cu^{I}(PTA)_n]^+$ and $Cu^{I}(A\beta)$ as a function of the Cu concentration

By considering only the predominant species $[Cu^{I}(PTA)_n]^+$ at a given concentration, the following equations can be used to evaluate the species present in the experiments performed.

General equations:

(A) (i)

Cu^{I} +	n PTA	→	$[Cu^{I}(PTA)_n]^+$
1	m		0
1-x	m-nx		x

$$\beta_{PTA,n} = \frac{[Cu(PTA)n]}{[PTA]^n[Cu]} = \frac{x}{(1-x)\left(1-\frac{n}{m}x\right)^n m^n {C_0}^n}$$

(ii) equilibrium between $[Cu^{I}(PTA)_n]^+$ and $[Cu^{I}(PTA)_{n-1}]^+$ complexes

Cu^{I} +	n PTA	→	$[Cu^{I}(PTA)_n]^+$
1	m		0
1-x-y	m-nx-(n-1)y		x

Cu^{I} +	(n-1) PTA	→	$[Cu^{I}(PTA)_{n-1}]^+$
1	m		0
1-x-y	m-nx-(n-1)y		y

$$\frac{\beta_{PTA,n-1}}{\beta_{PTA,n}} = \frac{[Cu(PTA)_{n-1}][Cu][PTA]^n}{[PTA]^{n-1}[Cu][Cu(PTA)_n]} = \frac{y\,[PTA]}{x} = \frac{(1-x)\,(m-n+1-x)C_0}{x}$$

(B)

Cu^{I} +	n PTA	→	$[Cu^{I}(PTA)_n]^+$
1	m		0
1-x-y	m-nx		x

Cu^{I} +	Aβ	→	$Cu^{I}(A\beta)$
1	1+ε		0
1-x-y	1+ε-y		y

$$\frac{K_{A\beta}}{\beta_{PTA,n}} = \frac{[PTA]^n[Cu]\,[Cu(A\beta)]}{[Cu(PTA)n][Cu][A\beta]} = \frac{m^n\left(1-\frac{n}{m}x\right)^n(y){C_0}^{n-1}}{(x)(1+\varepsilon-y)} = \frac{m^n\left(1-\frac{n}{m}x\right)^n(1-x){C_0}^{n-1}}{(x)(x+\varepsilon)}$$

(1) Spectroscopic characterizations of metal capture by the PTA ligands, [Cu] = 0.9 mM, [Aβ] = 1mM, number of PTA equivalent: 4 (for the coordination), species mainly present: $[Cu^{I}(PTA)_4]^+$ and Cu(Aβ).

Equation (B) with: $C_0 = 0.9\ 10^{-3}$ M, ε=0.11, m=n=4, and

$\frac{K_{A\beta}}{\beta_{PTA,4}} = 10^{-15}$ based on refs. [4] and [5], $[Cu(PTA)_4]^+$ = 0.88 mM, Cu(Aβ) = 0.02 mM

$\frac{K_{A\beta}}{\beta_{PTA,4}} = 10^{-12}$ based on refs. [6] and [5], $[Cu(PTA)_4]^+$ = 0.82 mM, Cu(Aβ) = 0.08 mM.

(2) ROS production experiments without Aβ

Equation (A) with: $C_0 = 10^{-5}$ M, m=4, n=3

$\frac{\beta_{PTA,2}}{\beta_{PTA,3}} =$ 10^{-6} based on ref. [5], $[Cu(PTA)_3]^+$ = 9.1 µM, $[Cu(PTA)_2]^+$ = 0.9 µM

(3) ROS production experiments: with Aβ

Equation (B) with: $C_0 = 10^{-5}$ M, ε=0.2, m=4, n=3,

$\frac{K_{A\beta}}{\beta_{PTA,3}} = 10^{-11}$ based on refs. [4] and [5] , $[Cu(PTA)_4]^+$ = 9.4 µM, Cu(Aβ) = 0.6 µM

$\frac{K_{A\beta}}{\beta_{PTA,3}} = 10^{-8}$ based on refs. [6] and [5], $[Cu(PTA)_4]^+$ = 3.3 µM, Cu(Aβ) = 6.7 µM

Depending on the values taken for the affinity of Cu(Aβ) in the literature reports, the speciation could be significantly different in case (3). Determination of the Cu(Aβ) affinity is beyond the scope of the present paper.

Note that for the above calculations, complexes with PTAH have not been taken into account since there only exist in acidic medium.

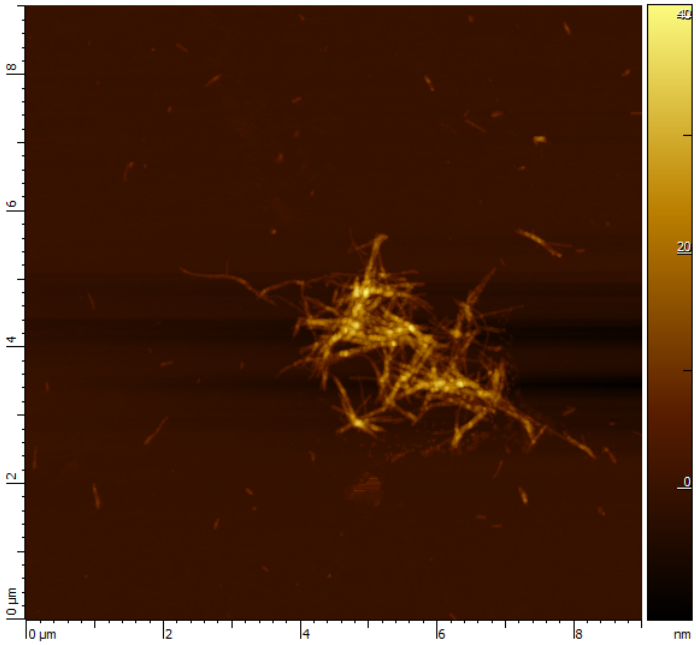
0 µm
2
4
6
8
nm
20
0

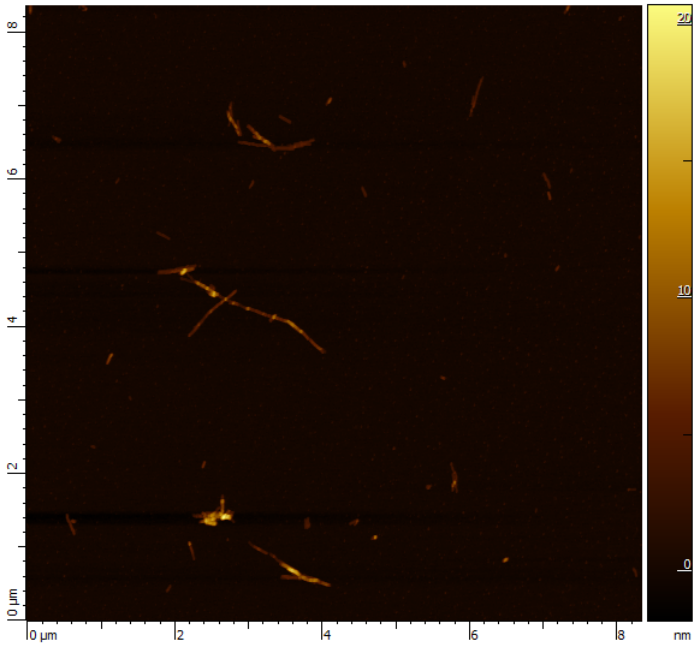
0 µm
2
4
6
8
nm
20
10
0

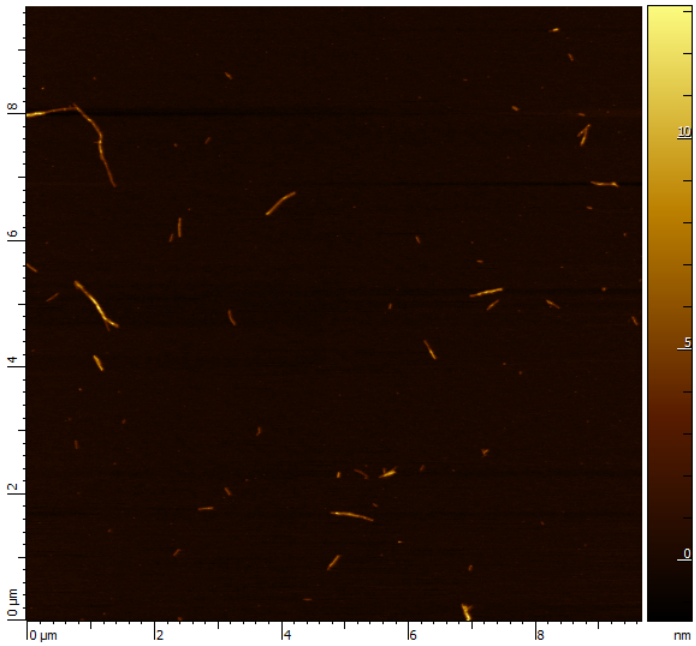
0 µm
2
4
6
8
nm
10
5
0

Cu^{II}-Aβ

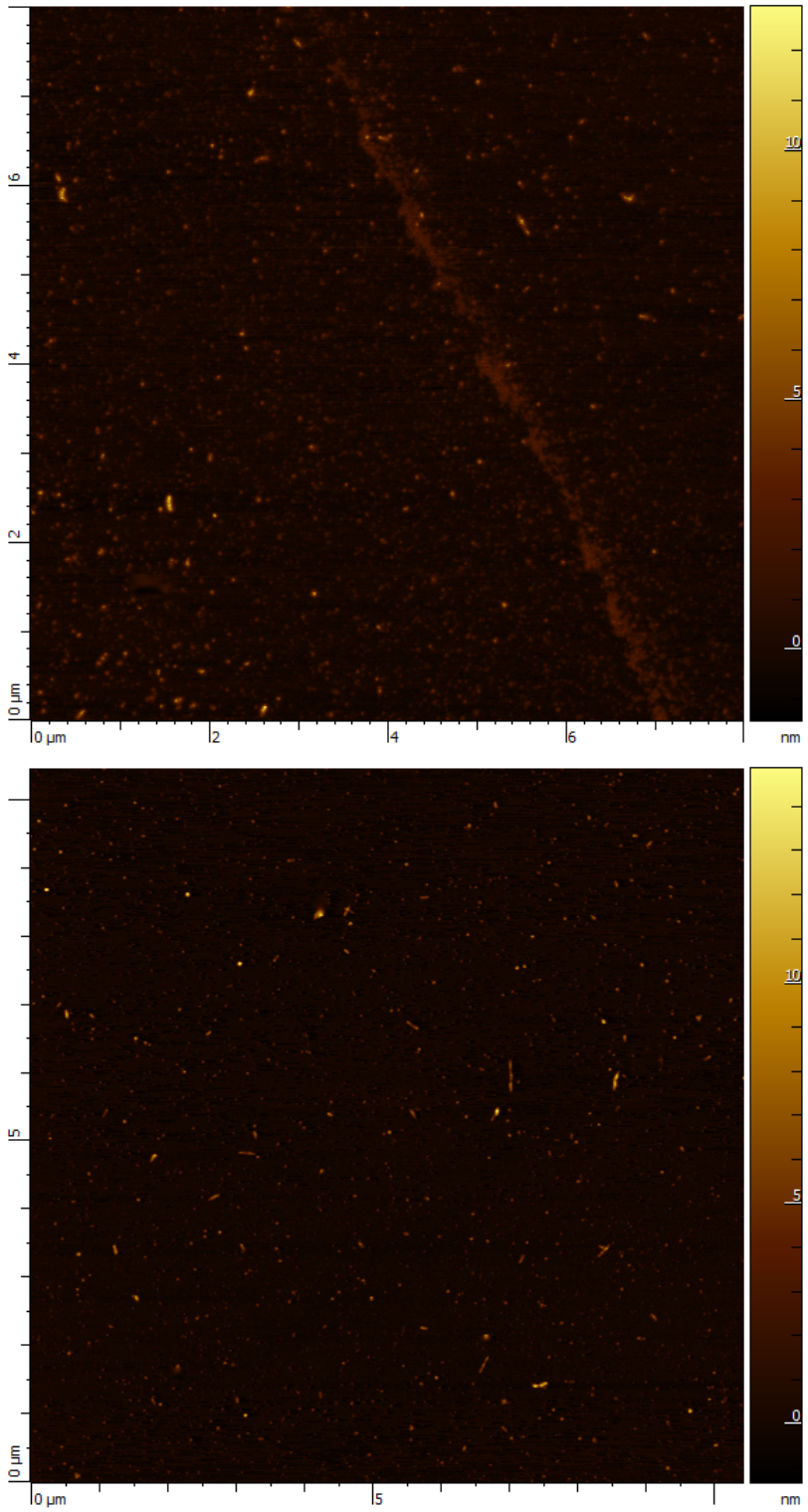

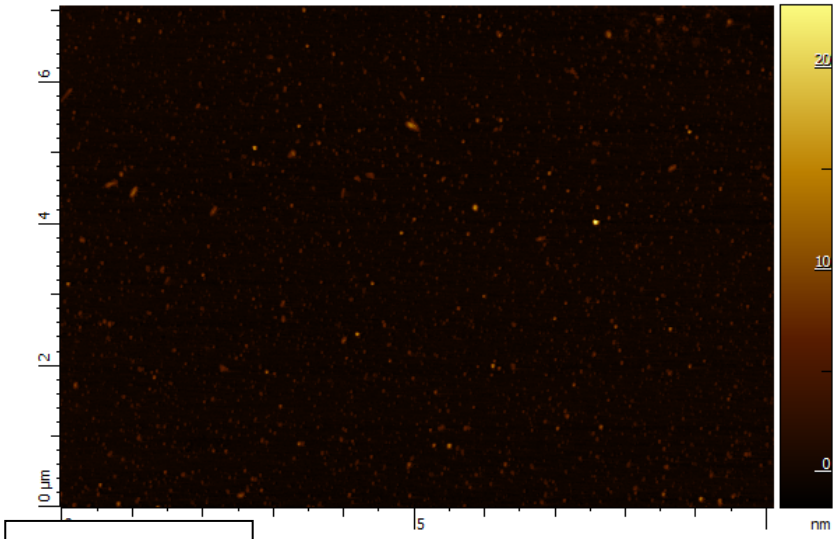

Cu^{II}-Aβ + 5 PTA

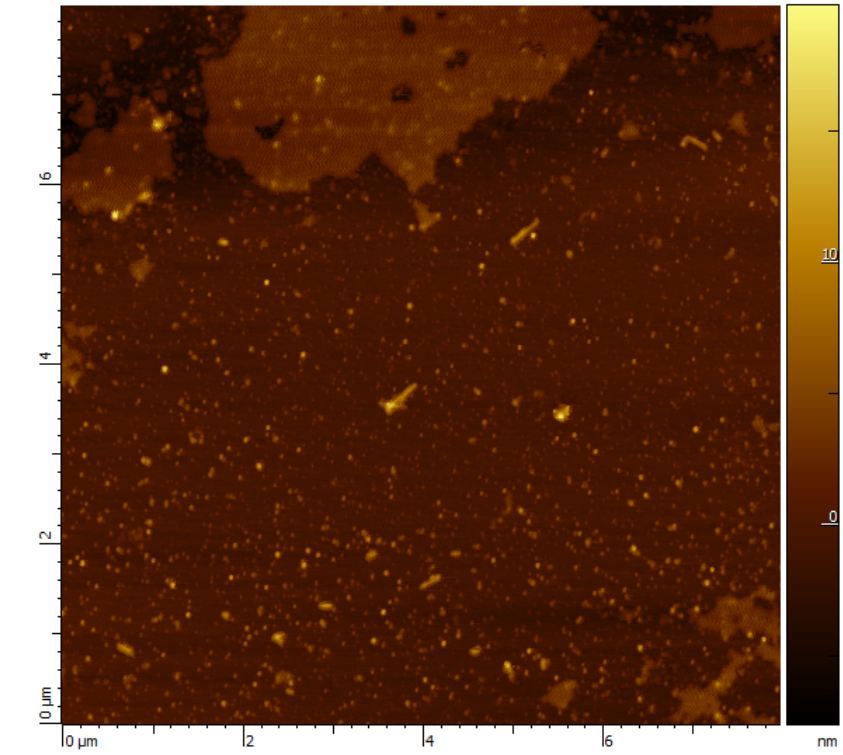

Cu^{II}-Aβ + 10 PTA

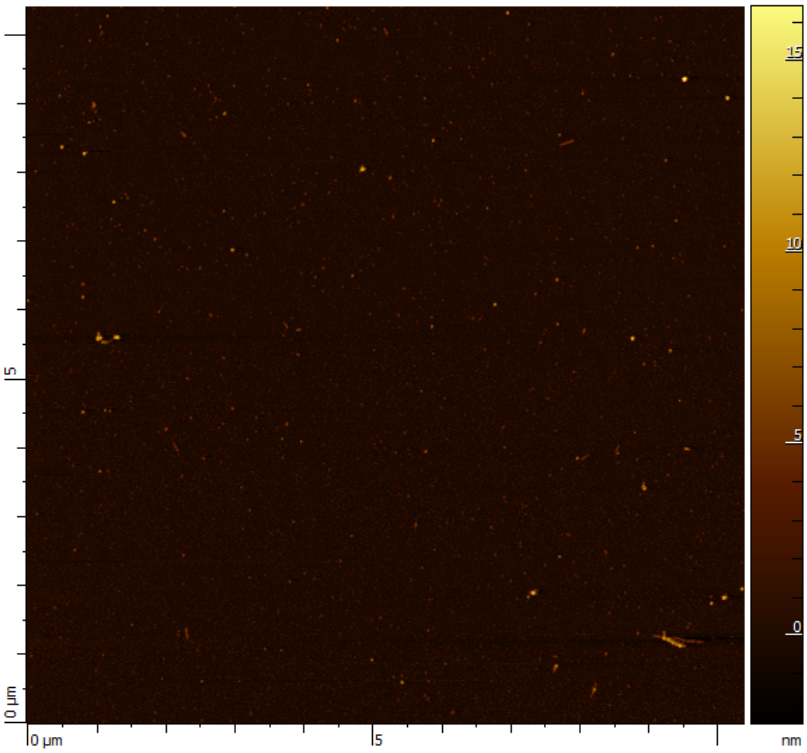

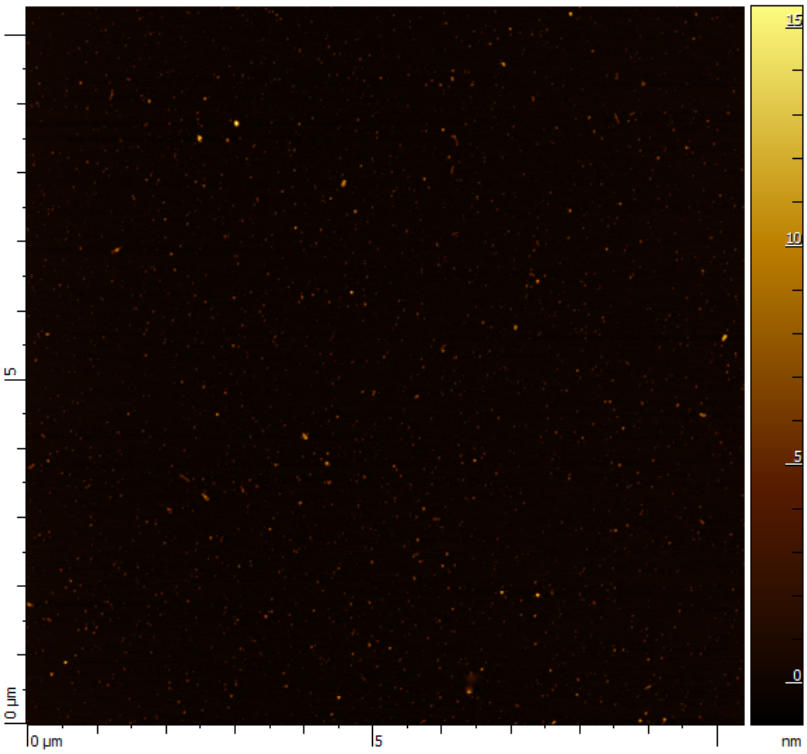

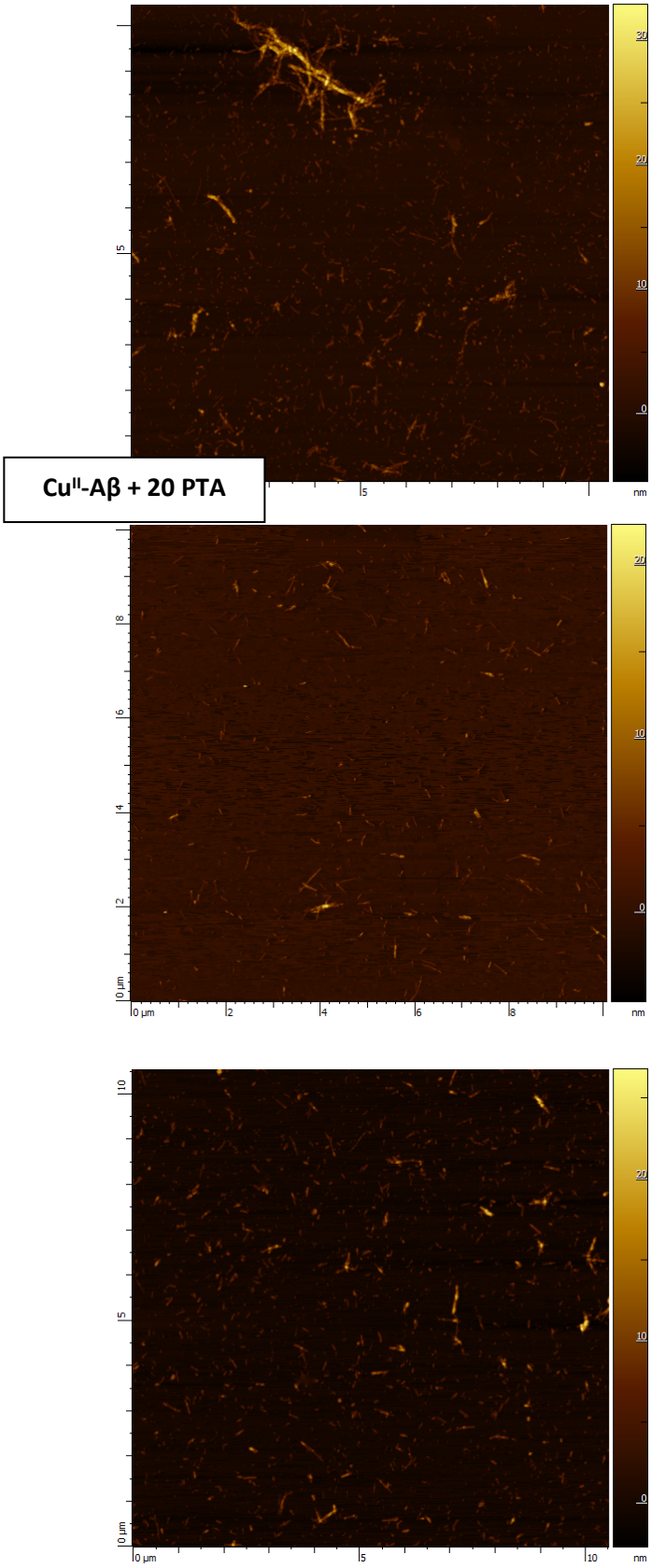

Figure S7. Selection of characteristic AFM pictures of 20µM Aβ40, Cu^{II}Aβ, Cu^{II}Aβ + 5 PTA, Cu^{II}Aβ + 10 PTA and Cu^{II}Aβ + 20 PTA following 180h of ThT fluorescence assay (T° = 37°C, pH = 7.0).

References.

1. P. Faller, C. Hureau, P. Dorlet, P. Hellwig, Y. Coppel, F. Collin and B. Alies, *Coord. Chem. Rev.*, 2012, **256**, 2381.
2. D. J. Daigle, T. J. Decuir, J. B. Robertson and D. J. Darensbourgh, *Inorg. Synth.*, 1998, **32**, 40.
3. C. Hureau, V. Balland, Y. Coppel, P. L. Solari, E. Fonda and P. Faller, *J. Biol. Inorg. Chem.*, 2009, 995.
4. B. Alies, B. Badei, P. Faller and C. Hureau, *Chem. Eur. J.*, 2012, **18**, 1161.
5. F. Endrizzi, *PhD thesis from the University of Padua*, 2013.
6. Z. Xiao, L. Gottschlich, R. van der Meulen, S. R. Udagedara and A. G. Wedd, *Metallomics*, 2013, **5**, 501.